
Zero-Shot Learning with Common Sense Knowledge Graphs

Nihal V. Nayak¹ Stephen H. Bach¹

Abstract

Zero-shot learning relies on semantic class representations such as hand-engineered attributes or learned embeddings to predict classes without any labeled examples. We propose to learn class representations from common sense knowledge graphs. Common sense knowledge graphs are an untapped source of explicit high-level knowledge that requires little human effort to apply to a range of tasks. To capture the knowledge in the graph, we introduce ZSL-KG, a general-purpose framework with a novel transformer graph convolutional network (TrGCN) for generating class representations. Our proposed TrGCN architecture computes non-linear combinations of the node neighbourhood and shows improvements on zero-shot learning tasks in language and vision. Our results show ZSL-KG outperforms the best performing graph-based zero-shot learning framework by an average of 2.1 accuracy points with improvements as high as 3.4 accuracy points. Our ablation study on ZSL-KG with alternate graph neural networks shows that our TrGCN adds up to 1.2 accuracy points improvement on these tasks.

1. Introduction

Zero-shot learning is a training strategy which allows a machine learning model to predict novel classes without the need for any labeled examples for the new classes (Romera-Paredes & Torr, 2015; Socher et al., 2013; Wang et al., 2019). These models learn parameters for the seen classes along with their class representations. During inference, new class representations are provided for the unseen classes. Previous zero-shot learning systems have used hand-engineered attributes (Akata et al., 2015; Farhadi et al., 2009; Lampert et al., 2014), pretrained embeddings (Frome et al., 2013) and learned embeddings (e.g., sentence embeddings) (Reed et al., 2016) as class representations.

Previous approaches for class representations have various

¹Department of Computer Science, Brown University, USA. Correspondence to: Nihal V. Nayak <nnayak2@cs.brown.edu>.

limitations. Attribute-based methods provide rich features and have achieved state-of-the-art results on several zero-shot object classification datasets, but the attributes have to be fixed ahead of time for the unseen classes and cannot adapt to new classes beyond the dataset. Furthermore, creating attribute datasets can take up to thousands of hours of labor (Zhao et al., 2019). Finally, attribute-based methods may not be readily applicable to tasks in language, as they might require greater nuance and flexibility (Gupta et al., 2020). Alternatively, pretrained embeddings such as GloVe (Pennington et al., 2014) and Word2Vec (Mikolov et al., 2013) offer the flexibility of easily adapting to new classes but rely on unsupervised training on large corpora—which may not provide distinguishing characteristics necessary for zero-shot learning. Many methods lie within this spectrum and learn class representations for zero-shot tasks from descriptions such as text and image prototypes.

Recently, there is growing interest in methods using graph neural networks on the ImageNet graph to learn to map nodes to class representations (Wang et al., 2018; Kampffmeyer et al., 2019). These graph-based methods have achieved strong performance on zero-shot object classification. They offer the benefits of high-level knowledge from the graph, with the flexibility of pre-trained embeddings. They are general-purpose and applicable to a broader range of tasks beyond object classification, since we show that they can be adapted to language datasets as well. However, the ImageNet graph is specialized to an object-type hierarchy, and may not provide rich features as suitable for a wide range of downstream tasks in multiple domains.

In our work, we propose to learn class representations better suited for a wider range of tasks from common sense knowledge graphs. Common sense knowledge graphs (Liu & Singh, 2004; Speer et al., 2017; Tandon et al., 2017; Zhang et al., 2020) are an untapped source of explicit high-level knowledge that requires little human effort to apply to a range of tasks. These graphs have explicit edges between related concept nodes and provide valuable information to distinguish between different concepts. However, adapting existing zero-shot learning frameworks to learn class representations from common sense knowledge graphs is challenging in several ways. GCNZ (Wang et al., 2018) learns graph neural networks with a symmetrically normalized graph Laplacian and requires the entire graph structure

during training, i.e., GCNZ is not inductive. Common sense knowledge graphs can be large (2 million to 21 million edges) and training a graph neural network on the entire graph can be prohibitively expensive. DGP (Kampffmeyer et al., 2019) is an inductive method and aims to generate expressive class representations, but assumes a directed acyclic graph such as ImageNet. Common sense knowledge graphs do not have a directed acyclic graph structure.

To address these limitations, we propose ZSL-KG, a framework with a novel transformer graph convolutional network (TrGCN) to learn class representations. Graph neural networks learn to represent the structure of graphs by aggregating information from each node’s neighbourhood. Aggregation techniques used in GCNZ, DGP, and most other graph neural network approaches are linear, in the sense that they take a (possibly weighted) mean or maximum of the neighbourhood features. To capture the complex information in the common sense knowledge graph, TrGCN learns a transformer-based aggregator to compute a non-linear combination of the node neighbours. A few prior works have used LSTMs as non-linear aggregators (Hamilton et al., 2017a) as a way to increase the expressivity of graph neural networks, but their outputs can be sensitive to the ordering imposed on the nodes in each neighborhood. In contrast, TrGCN learns a transformer-based aggregator, which is non-linear and naturally permutation invariant. Additionally, our framework is inductive, i.e., the graph neural network can be executed on graphs that are different from the training graph, which is necessary for generalized zero-shot learning under which the test classes are unknown during training.

We demonstrate the effectiveness of our framework on two generalized zero-shot learning tasks with five datasets in language and vision: fine-grained entity typing and object classification. Our results show ZSL-KG outperforms the best performing graph-based zero-shot learning framework by an average of 2.1 accuracy points with improvements as high as 3.4 accuracy points on five benchmark datasets including the large-scale ImageNet 22k dataset. In summary, our main contributions are the following:

1. We propose to learn to map nodes in common sense knowledge graphs to class representations for zero-shot learning.
2. We present ZSL-KG, a framework based on graph neural networks with a novel transformer graph convolutional network (TrGCN). Our proposed architecture learns permutation invariant non-linear combinations of the nodes’ neighbourhoods and generates expressive class representations.
3. ZSL-KG achieves new state-of-the-art accuracies for generalized zero-shot learning on the OntoNotes (Gillick et al., 2014), BBN (Weischedel & Brunstein, 2005), and attribute Pascal Yahoo (aPY) (Farhadi et al., 2009) datasets. ZSL-KG also outperforms existing

graph-based zero-shot learning frameworks on the ImageNet 22K dataset (all classes used for testing) (Deng et al., 2009), while maintaining competitive performance on Animals with Attributes 2 (AWA2) dataset (Xian et al., 2018). We are also the first to demonstrate that graph-based zero-shot learning frameworks—originally designed for object classification—are also applicable to language tasks.

2. Background

In this section, we summarize zero-shot learning and graph neural networks.

2.1. Zero-Shot Learning

Zero-shot learning has several variations (Wang et al., 2019). We focus on generalized zero-shot learning (GZSL). GZSL is the most challenging and reflects the real-world setting where we have both seen and unseen classes during testing (Xian et al., 2018). Formally, we have the training set $\mathbb{S} = \{(x_1, y_1), \dots, (x_n, y_n)\}$ where $y_n \in Y_S$ belongs to the seen classes. During test time, our objective is to assign examples to the correct class(es) from both seen and unseen classes i.e. $y_n \in Y_{U+S}$ where Y_U is the set of unseen classes and $Y_S \cap Y_U = \emptyset$.

We train a zero-shot classifier by optimizing over the seen classes. But, unlike traditional methods, zero-shot classifiers are trained along with class representations such as attributes, pretrained embeddings, etc. Recent approaches learn a class encoder $\phi(y) \in \mathbb{R}^d$ to produce vector-valued class representations from an initial input, such as a string or other identifier of the class. (In our case, y is a node in a graph and its k -hop neighborhood.) During inference, the class representations are used to label examples with the unseen classes by passing the examples through an example encoder $\theta(x) \in \mathbb{R}^d$ and predicting the class whose representation has the highest inner product with the example representation.

Recent work in zero-shot learning commonly uses one of two approaches to learn the class encoder $\phi(y)$. One approach uses a bilinear similarity function defined by a compatibility matrix $\mathbf{W} \in \mathbb{R}^{d \times d}$ (Frome et al., 2013; Xian et al., 2018):

$$f(\theta(x), \mathbf{W}, \phi(y)) = \theta(x)^T \mathbf{W} \phi(y). \quad (1)$$

The bilinear similarity function gives a score for each example-class pair. The parameters of θ , \mathbf{W} , and ϕ are learned by taking a softmax over f for all possible seen classes $y \in Y_S$ and minimizing either the cross entropy loss or a ranking loss with respect to the true labels. In other words, f should give a higher score for the correct class(es) and lower scores for the incorrect classes. \mathbf{W} is

often constrained to be low rank, to reduce the number of learnable parameters (Obeidat et al., 2019; Yogatama et al., 2015). Lastly, other variants of the similarity function add minor variations such as non-linearities between factors of W (Xian et al., 2016).

The other common approach is to first train a neural network classifier in a supervised fashion. The final fully connected layer of this network has a vector representation for each seen class, and the remaining layers are used as the example encoder $\theta(x)$. Then, the class encoder $\phi(y)$ is trained by minimizing the L2 loss between the representations from supervised learning and $\phi(y)$ (Socher et al., 2013; Wang et al., 2018). The class encoder that we propose in Section 3 can be plugged into either approach.

2.2. Graph Neural Networks

The basic idea behind graph neural networks is to learn node embeddings that reflect the structure of the graph (Hamilton et al., 2017b). Consider the graph $\mathcal{G} = (V, E, R)$, where V is the set of vertices with node features X_v and $(v_i, r, v_j) \in E$ are the labeled edges and $r \in R$ are the relation types. Graph neural networks learn node embeddings by iterative aggregation of the k-hop neighbourhood. Each layer of a graph neural network has two main components AGGREGATE and COMBINE (Xu et al., 2019):

$$\mathbf{a}_v^{(l)} = \text{AGGREGATE}^{(l)} \left(\left\{ \mathbf{h}_u^{(l-1)} \forall u \in \mathcal{N}(v) \right\} \right) \quad (2)$$

where $\mathbf{a}_v^{(l)} \in \mathbb{R}^{d_{l-1}}$ is the aggregated node feature of the neighbourhood, $\mathbf{h}_u^{(l-1)}$ is the node feature in neighbourhood $\mathcal{N}(\cdot)$ of node v including a self loop. The aggregated node is passed to the COMBINE to generate the node representation $\mathbf{h}_v^{(l)} \in \mathbb{R}^{d_l}$ for the l -th layer:

$$\mathbf{h}_v^{(l)} = \text{COMBINE}^{(l)} \left(\mathbf{h}_v^{(l-1)}, \mathbf{a}_v^{(l)} \right) \quad (3)$$

$\mathbf{h}_v^{(0)} = \mathbf{x}_v$ where \mathbf{x}_v is the initial feature vector for the node. Previous works on graph neural networks for zero-shot learning have used GloVe (Pennington et al., 2014) to represent the initial features (Wang et al., 2018).

Hamilton et al. (2017a) proposed using LSTMs as non-linear aggregators. However, their outputs can be sensitive to the order of the neighbours in the input sequence. For example, on the Animals with Attributes 2 dataset, we find that when given the same test image 10 times with different neighbourhood orderings, an LSTM-based graph neural network outputs inconsistent predictions 16% of the time (Appendix A). One recent work considers trying to make LSTMs less sensitive by averaging the outputs over permutations, but this significantly increases the computational cost and provides only a small boost to prediction accuracy (Murphy et al., 2019). In contrast, our proposed TrGCN in ZSL-KG is non-linear and naturally permutation invariant.

3. The ZSL-KG Framework

Here we introduce ZSL-KG: a framework with a novel transformer graph convolutional network (TrGCN) to learn class representation from common sense knowledge graphs. Figure 1 shows the ZSL-KG architecture with an example elephant concept.

3.1. Common Sense Knowledge Graphs for ZSL

Common sense knowledge graphs organize high-level knowledge implicit to humans in a graph. The nodes in the graph are concepts associated with each other via edges. As we show in our work, these associations in the graph offer a rich and a large-scale source of high-level information, which makes them applicable to a wide range of tasks. To learn class representations, we look to existing zero-shot learning frameworks with graph neural networks. Existing zero-shot learning frameworks such as GCNZ (Wang et al., 2018) and DGP (Kampffmeyer et al., 2019) that learn class representations from structured knowledge are applicable only to small graphs like ImageNet or Wordnet as they make restrictive assumptions. First, GCNZ requires access to the entire graph during training. Since publicly available common sense knowledge graphs range roughly from 100,000 to 8 million nodes and 2 million to 21 million edges (Speer et al., 2017; Zhang et al., 2020), this makes training computationally difficult. Further, with inductive tasks like generalized zero-shot learning, the graph may change at test time as new classes are added. Second, DGP requires a directed acyclic graph or parent-child relationship in the graph. In a common sense knowledge graph, we are not restricted to parent-child relationships.

3.2. Transformer Graph Convolutional Networks

To overcome these limitations, we propose to learn class representations with a novel graph neural network: transformer graph convolutional networks (TrGCN). Transformers (Vaswani et al., 2017) are non-linear modules typically used for machine translation and language modeling tasks. They achieve a non-linear combination of the input sets using two-layer feedforward neural networks and self attention. We exploit this property to learn a permutation invariant non-linear aggregator that captures the complex structure of a common sense knowledge graph. Finally, the learned model can be used to predict with new graph structures without retraining which makes them well suited for generalized zero-shot learning.

Here we describe TrGCN. We pass the neighbourhood node features $\mathbf{h}_u^{(l-1)}$ through a two-layer feedforward neural network with a ReLU activation between the layers. The previous features are added to its output features with a skip connection, followed by layer normalization (LN) (Ba et al.,

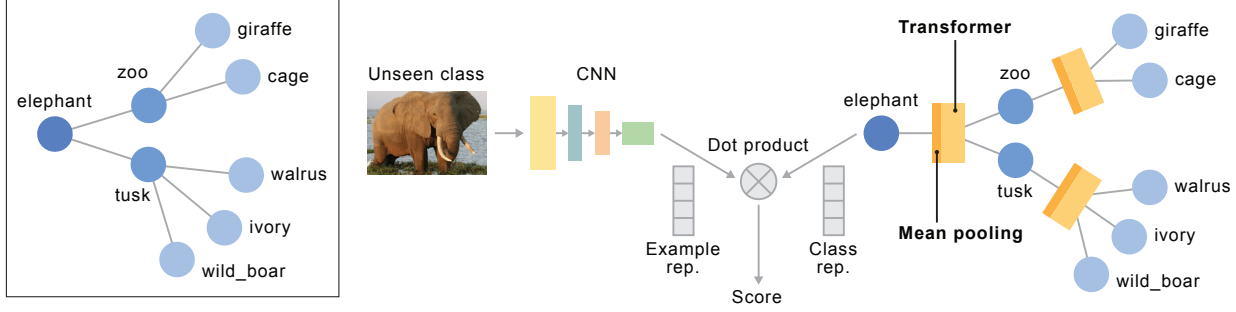


Figure 1. *Left*: A sample from the 2-hop neighbourhood for the concept `elephant` from ConceptNet. *Right*: The ZSL-KG architecture. The image of an elephant is passed through the example encoder (ResNet101) to generate the example representation. For the class representation, we take the sampled k-hop neighbourhood and pass the nodes through their hop-specific transformer graph convolutional network (TrGCN). The same architecture is used for language tasks with a task-specific example encoder.

2016):

$$\mathbf{h}_u^{(l-1)} = \text{LN} \left\{ \mathbf{W}_{fh}^{(l)} \left[\sigma \left(\mathbf{W}_{hf}^{(l)} \mathbf{h}_u^{(l-1)} \right) \right] + \mathbf{h}_u^{(l-1)} \right\} \quad (4)$$

where $\mathbf{W}_{hf}^{(l)} \in \mathbb{R}^{d_{(l-1)} \times d_{(f)}}$ and $\mathbf{W}_{fh}^{(l)} \in \mathbb{R}^{d_{(f)} \times d_{(l-1)}}$ are learnable weight matrices for the feedforward neural network and $\sigma(\cdot)$ is ReLU activation. The non-linear neighbourhood features are then passed through the self attention layer to compute the weighted combination of the features for each query node:

$$\left\{ \mathbf{z}_u^{(l)} \forall u \in \mathcal{N}(v) \right\} = \text{softmax} \left(\frac{\mathbf{Q}\mathbf{K}^T}{\sqrt{d_{(p)}}} \right) \mathbf{V} \quad (5)$$

where $\mathbf{Q} = \mathbf{W}_q^{(l)} \mathbf{h}_u^{(l-1)}$ is the set of all neighbourhood query vectors, $\mathbf{K} = \mathbf{W}_k^{(l)} \mathbf{h}_u^{(l-1)}$ is the set of all key vectors, $\mathbf{V} = \mathbf{W}_v^{(l)} \cdot \mathbf{h}_u^{(l-1)}$ is the set of values vectors, and $\mathbf{W}_q \in \mathbb{R}^{d_{(l-1)} \times d_{(p)}}$, $\mathbf{W}_k \in \mathbb{R}^{d_{(l-1)} \times d_{(p)}}$, $\mathbf{W}_v \in \mathbb{R}^{d_{(l-1)} \times d_{(p)}}$ are learnable weight matrices with the projection dimension $d_{(p)}$. The output features from the attention layer is projected with another linear layer and added to its previous features with a skip connection, followed by layer normalization:

$$\left\{ \mathbf{z}_u^{(l)} \forall u \in \mathcal{N}(v) \right\} = \text{LN} \left(\mathbf{W}_z^{(l)} \mathbf{z}_u^{(l-1)} + \mathbf{h}_u^{(l-1)} \right) \quad (6)$$

where $\mathbf{W}_z^{(l)} \in \mathbb{R}^{d_{(p)} \times d_{(l-1)}}$ is a learnable weight matrix.

To get the aggregated vector $\mathbf{a}_v^{(l)}$ for node v , we pass the output vectors $\{\mathbf{z}_u^{(l)} \forall u \in \mathcal{N}(v)\}$ from the transformer through a permutation invariant pooling function $\mu(\cdot)$ such as mean-pooling. The aggregated vector is passed through a linear layer followed by a non-linearity $\sigma(\cdot)$ such as ReLU or LeakyReLU:

$$\mathbf{a}_v^{(l)} = \mu \left(\left\{ \mathbf{z}_u^{(l)} \forall u \in \mathcal{N}(v) \right\} \right) \quad \mathbf{h}_v^{(l)} = \sigma \left(\mathbf{W}^{(l)} \cdot \mathbf{a}_v^{(l)} \right) \quad (7)$$

where $\mathbf{W}^{(l)} \in \mathbb{R}^{d_{(l-1)} \times d_{(l)}}$ is a learnable weight matrix.

Existing work has drawn parallels between transformers and graph attention networks (GAT), suggesting that they are equivalent (Joshi, 2020). The work shows GAT is equivalent to transformers if the graph is treated as fully connected. Our proposed TrGCN differs from GAT in two ways: (1) the transformer-based aggregator computes the non-linear combination of the input features by passing it through the two-layer feedforward neural network and the self attention whereas GAT only computes a linear combination of the node features (2) the aggregated vector is computed by passing the features after the self attention through an additional pooling function, which is equivalent to treating the node’s neighbours as a fully connected graph. Finally, in section 4.4, we show that the non-linear aggregator is the key difference between GAT and TrGCN.

Neighbourhood Sampling. In our experiments, we use ConceptNet (Speer et al., 2017) as our common sense knowledge graph, but ZSL-KG is agnostic to the choice of the knowledge graph. ConceptNet has high node degree, which poses a challenge to train the graph neural network. To solve this problem, we explored numerous neighbourhood sampling strategies. Existing work on sampling neighbourhood includes random sampling (Hamilton et al., 2017a), importance sampling (Chen et al., 2018a), random walks (Ying et al., 2018), etc. Similar to PinSage (Ying et al., 2018), we simulate random walks for the nodes in the graph and assign hitting probabilities to the neighbourhood nodes. During training and testing the graph neural network, we select the top N nodes from the neighbourhood based on their hitting probability.

Stacked Calibration. In generalized zero-shot learning setting, we predict both seen and unseen classes. However, generalized ZSL models tend to overpredict the seen classes (Chao et al., 2016). Following prior work (Xu et al., 2020), we solve this issue by simply lowering the compatibility

	<i>OntoNotes</i>			<i>BBN</i>			Overall
	Strict Acc.	Loose Mic.	Loose Mac.	Strict Acc.	Loose Mic.	Loose Mac.	Strict Avg.
GCNZ	41.46 ± 0.81	54.61 ± 0.52	61.65 ± 0.52	21.47 ± 1.22	47.17 ± 1.04	56.81 ± 0.68	31.47
SGCN	42.64 ± 0.69	56.25 ± 0.29	62.93 ± 0.39	24.91 ± 0.24	50.02 ± 0.73	59.68 ± 0.54	33.77
DGP	41.11 ± 0.78	54.08 ± 0.62	61.38 ± 0.76	23.99 ± 0.14	47.19 ± 0.51	57.62 ± 0.89	32.55
ZSL-KG	45.21 ± 0.36	55.81 ± 0.41	63.64 ± 0.51	26.69 ± 2.41	50.30 ± 1.21	57.66 ± 1.15	35.95

Table 1. The results for generalized zero-shot fine-grained entity typing on Ontonotes and BBN. We report the average strict accuracy, loose micro F1, and loose macro F1 of the models on 5 random seeds and the standard error.

scores for the seen classes:

$$f(\theta(x), \mathbf{W}, \phi(y_i)) = f(\theta(x), \mathbf{W}, \phi(y_i)) - \gamma \mathbf{1}_{y_i \in Y_S} \quad (8)$$

where the calibration coefficient $\gamma \in \mathbb{R}$ is a hyperparameter tuned on the held-out validation set.

4. Tasks and Results

We evaluate our framework on two generalized zero-shot learning tasks: fine-grained entity typing and object classification. In all our experiments, we compare ZSL-KG with graph-based methods: GCNZ, SGCN, and DGP.

GCNZ (Wang et al., 2018) uses symmetrically normalized graph Laplacian to generate the class representations. SGCN, introduced as a baseline in Kampffmeyer et al. (2019), uses an asymmetrical normalized graph Laplacian to learn the class representations. Finally, DGP (Kampffmeyer et al., 2019) uses a dense graph connectivity scheme with a two-stage propagation from ancestors and descendants to learn the class representations.

In each task, we also evaluate ZSL-KG against the specialized state-of-the-art methods. These methods are considered specialized because they either cannot easily be adapted to multiple domains (e.g., attribute-based methods cannot easily be adapted to language dataset) or require greater human effort to make them applicable to other domains (e.g., mapping ImageNet to Wikipedia articles).

Setup. We use two-layer graph neural networks for the graph-based methods and ZSL-KG. We mapped the classes to the nodes in the WordNet graph for each dataset and use the code obtained from Kampffmeyer et al. (2019) to adapt the methods to language datasets. We provide details related to the mapping of classes to ConceptNet, post-processing ConceptNet, sampling, and random walk details in Appendix B and the pseudocode for ZSL-KG in Appendix C. Additional task-specific details are below.

4.1. Fine-Grained Entity Typing

Fine-grained entity typing is the task of categorizing the entities of a sentence into one or more narrowly scoped

semantic types. The ability to identify novel fine-grained types without additional human effort would benefit the several downstream tasks in relation extraction (Yaghoobzadeh & Schütze, 2015), question answering (Yavuz et al., 2016), and coreference resolution (Durrett & Klein, 2014).

Datasets. Fine-grained entity typing is a zero-shot multi-label classification task because each entity can be associated with more than one type. We evaluate on popular fine-grained entity typing datasets: OntoNotes (Gillick et al., 2014) and BBN (Weischedel & Brunstein, 2005). We split the dataset into two: coarse-grained labels (e.g., /location) and fine-grained labels (e.g., /location/city). See Appendix D for more details on the datasets. Following the prior work (Obeidat et al., 2019), we train on the coarse-grained labels and predict on both coarse-grained and fine-grained labels in the test set.

	<i>OntoNotes</i>	<i>BBN</i>
	Strict	Strict
OTyper	41.72 ± 0.44	25.76 ± 0.25
DZET	42.88 ± 0.47	26.20 ± 0.13
ZSL-KG	45.21 ± 0.36	26.69 ± 2.41

Table 2. The results for generalized zero-shot learning on OntoNotes and BBN with specialized state-of-the-art methods. We report the average strict accuracy of the models on 5 random seeds and the standard error.

Experiment. We use a bilinear similarity function (Eq. 1) for ZSL-KG and the graph-based methods. The example encoder is AttentiveNER biLSTM (Shimaoka et al., 2017) (see Appendix G) and the class encoder is the graph neural network. We also reconstruct the specialized state-of-the-art methods for task: OTyper (Yuan & Downey, 2018), and DZET (Obeidat et al., 2019). OTyper uses average word embeddings and DZET uses Wikipedia Descriptors as their class representations. The methods are trained by minimizing the cross-entropy loss. For more details on the experiment, training, and inference see Appendix E.1.

As is common for this task (Obeidat et al., 2019), we evaluate the performance of our model on strict accuracy, loose micro F1, and loose macro F1 (Appendix H). Strict accuracy

Zero-Shot Learning with Common Sense Knowledge Graphs

		Hit@k(%)														
		2-Hops					3-Hops					All				
		1	2	5	10	20	1	2	5	10	20	1	2	5	10	20
ZSL	GCNZ	19.8	33.3	53.2	65.4	74.6	4.1	7.5	14.2	20.2	27.7	1.8	3.3	6.3	9.1	12.7
	SGCN	26.2	40.4	60.2	71.9	81.0	6.0	10.4	18.9	27.2	36.9	2.8	4.9	9.1	13.5	19.3
	DGP	26.6	40.7	60.3	72.3	81.3	6.3	10.7	19.3	27.7	37.7	3.0	5.0	9.3	13.9	19.8
	ZSL-KG	26.3	40.6	60.3	71.9	81.2	6.3	11.1	20.1	28.8	38.8	3.0	5.3	9.9	14.8	21.0
GZSL	GCNZ	9.7	20.4	42.6	57.0	68.2	2.2	5.1	11.9	18.0	25.6	1.0	2.3	5.3	8.1	11.7
	SGCN	11.9	27.0	50.8	65.1	75.9	3.2	7.1	16.1	24.6	34.6	1.5	3.4	7.8	12.3	18.2
	DGP	10.3	26.4	50.3	65.2	76.0	2.9	7.1	16.1	24.9	35.1	1.4	3.4	7.9	12.6	18.7
	ZSL-KG	11.1	26.2	50.0	64.3	75.3	3.4	7.5	16.9	26.1	36.5	1.7	3.8	8.5	13.5	19.9

Table 3. Results for object classification on ImageNet dataset. We report the class-balanced top-k accuracy on zero-shot learning (ZSL) and generalized zero-shot learning (GZSL) for ImageNet classes k-hops away from the ILSVRC 2012 classes. The results for GCNZ, SGCN, and DGP are obtained from [Kampffmeyer et al. \(2019\)](#).

penalizes the model for incorrect label predictions and the number of the label predictions have to match the ground truth, whereas loose micro F1 and loose macro F1 measures if the correct label is predicted among other false positive predictions.

Results. Table 1 shows that, on average, ZSL-KG outperforms the best performing graph-based method (SGCN) by 2.18 strict accuracy points. SGCN has higher loose micro on OntoNotes and loose macro on BBN datasets because it overpredicts labels and has greater false positives compared to the ZSL-KG. Our method has higher precision for label predictions and therefore, higher strict accuracy compared to other methods. Table 2 shows that ZSL-KG outperforms the specialized baselines and achieves the new state-of-the-art on the task.

4.2. Object Classification

Object classification is a computer vision task of categorizing objects into different class categories.

Datasets. Zero-shot object classification is a multiclass classification task. We evaluate our method on the large-scale ImageNet ([Deng et al., 2009](#)), Attributes 2 (AWA2) ([Xian et al., 2018](#)), and attribute Pascal Yahoo (aPY) ([Farhadi et al., 2009](#)) datasets. See Appendix D for more details on the datasets.

Experiment. Following prior work ([Kampffmeyer et al., 2019](#); [Wang et al., 2018](#)), we learn class representations by minimizing the L2 distance between the learn class representations and the weights of the fully connected layer of a ResNet classifier pretrained on the ILSVRC 2012. Next, we freeze the class representations and finetune the ResNet-backbone on the training images from the dataset. More details on the experiments are included in Appendix E.2.

Following prior work ([Kampffmeyer et al., 2019](#)), we evaluate ImageNet on two settings: zero-shot learning (ZSL) where the model predicts only unseen classes and generalized zero-shot learning (GZSL) where the model predicts both seen and unseen classes. We follow the train/test split from [Frome et al. \(2013\)](#), and evaluate ZSL-KG on three levels of difficulty: 2-hops (1549 classes), 3-hops (7860 classes), and All (20842 classes). The hops refer to the distance of the classes from the ILSVRC train classes. We report the class-balanced top-K (Hit@k) accuracy for each of the hops.

We evaluate AWA2 and aPY in the ZSL and GZSL settings as well. Following prior work ([Xian et al., 2018](#)), for ZSL, we use the pretrained ResNet101 as the backbone and report the class-balanced accuracy on the unseen classes (T1). Similarly ([Min et al., 2020](#)), for GZSL, we use the finetuned ResNet101 to report the class-balanced accuracy on the unseen classes (U), seen classes (S), and their harmonic mean (H).

Results. Table 3 shows results for ImageNet dataset. ZSL-KG, despite being trained on a noisier graph, achieves competitive performance on the ImageNet dataset on both ZSL and GZSL settings. ZSL-KG outperforms graph-based methods on 3-hops (7860 classes) and All (20842 classes) for ZSL and GZSL evaluation. Table 4 shows that ZSL-KG, on average, achieves significantly higher harmonic mean than the graph-based methods on AWA2 and aPY. We also observe that the graph-based methods show a significant drop in accuracy from AWA2 to aPY, whereas our method consistently achieves high accuracy on both the datasets. Table 5 shows ZSL-KG compared with specialized attribute-based methods. ZSL-KG outperforms the state-of-the-art on aPY dataset by 14.0 points on harmonic mean and achieves an average improvement of 7.3 points on the harmonic mean for both the datasets. We suspect that pretraining ZSL-KG

Zero-Shot Learning with Common Sense Knowledge Graphs

	AWA2				aPY				Overall
	T1	U	S	H	T1	U	S	H	Avg. H
GCNZ	77.00 ± 2.05	66.62 ± 1.28	81.63 ± 0.18	73.30 ± 0.75	51.66 ± 0.74	49.11 ± 0.39	71.26 ± 0.20	58.14 ± 0.29	65.74
SGCN	77.10 ± 1.49	67.51 ± 1.29	81.16 ± 0.11	73.67 ± 0.74	52.32 ± 0.37	47.29 ± 0.63	71.05 ± 0.18	56.78 ± 0.47	65.23
DGP	77.10 ± 1.33	71.26 ± 1.02	79.39 ± 0.09	75.09 ± 0.61	49.73 ± 0.30	46.16 ± 0.66	70.16 ± 0.25	55.68 ± 0.52	65.38
ZSL-KG	78.08 ± 0.84	66.80 ± 0.70	84.42 ± 0.33	74.58 ± 0.53	60.54 ± 0.58	55.16 ± 0.50	69.66 ± 0.52	61.57 ± 0.45	68.07

Table 4. Results for generalized zero-shot object classification on the AWA2 and aPY dataset. We report the average class-balanced accuracy of the models for ZSL (T1) and GZSL (U, S, H) on 5 random seeds and the standard error.

	AWA2				aPY			
	T1	U	S	H	T1	U	S	H
ZSML	77.5	58.9	74.6	65.8	64.0	36.3	46.6	40.9
IPN	-	67.5	79.2	72.9	-	37.2	66	47.6
AGZSL	76.4	69.0	86.5	76.8	43.7	36.2	58.6	44.8
ZSL-KG	78.1	66.8	84.4	74.6	60.5	55.2	69.7	61.6

Table 5. Results for generalized zero-shot object classification on the AWA2 and aPY dataset with best performing specialized methods. The results for ZSML (Verma et al., 2020), AGZSL (Chou et al., 2021), and IPN (Liu et al., 2021) are obtained from their manuscripts. For extended results with other specialized methods, see Appendix I.

class representations on ILSVRC 2012 classes helps the performance. Existing attribute-based methods cannot be pretrained on ILSVRC because ILSVRC does not have hand-crafted attributes. This highlights potential benefits of using class representations from graphs.

4.3. Discussion

Our results on fine-grained entity typing show that ZSL-KG achieves the highest strict accuracy compared to the graph-based methods on both OntoNotes and BBN datasets. On object classification, we see that no one method dominates in all the three datasets. We observe that DGP does well on AWA2, but it performs relatively poorly on ImageNet and aPY datasets in generalized zero-shot learning. In contrast, we see that ZSL-KG achieves the highest performance on larger sets of ImageNet and reports new state-of-the-art for aPY, while maintaining competitive performance on AWA2 dataset. Finally, averaging the strict accuracy on OntoNotes and BBN, harmonic mean on AWA2 and aPY, and Top-1 GZSL for all classes on ImageNet, we observe that ZSL-KG outperforms the best performing graph-based method (SGCN) by an average of 2.1 accuracy points and all the graph-based methods’ accuracies by an average of 1.5 accuracy points. These results demonstrate the superior flexibility and generality of ZSL-KG to achieve competitive performance on both language and vision tasks.

4.4. Comparison of Graph Aggregators

We conduct an ablation study with different aggregators with our framework. Existing graph neural networks include GCN (Kipf & Welling, 2017), GAT (Veličković et al., 2018), RGCN (Schlichtkrull et al., 2018) and LSTM (Hamilton et al., 2017a). We provide all the architectural details in Appendix K. We train these models with the same experimental setting for the tasks mentioned in their respective sections.

Results. Table 6 shows results for our ablation study. Our results show that TrGCN often outperforms existing graph neural networks with linear aggregators and TrGCN adds up to 1.23 accuracy points improvement on these tasks. No architecture is superior on all tasks, but TrGCN is the best on a majority of them.

It is also worth comparing SGCN and ZSL-KG-GCN, as they use the same linear aggregator to learn the class representation but train with different knowledge graphs. We see that ZSL-KG-GCN trained on common sense knowledge graphs adds an improvement as high as 3.7 accuracy points across the tasks suggesting that the choice of knowledge graphs is crucial for downstream performance.

	OntoNotes	BBN	AWA2	aPY	ImageNet
	Strict	Strict	H	H	All (%)
ZSL-KG	45.21	26.69	74.58	61.57	1.74
-GCN	42.19	27.44	73.08	60.45	1.78
-GAT	43.48	32.65	73.35	60.91	1.77
-RGCN	43.88	27.89	47.96	31.60	—
-LSTM	44.52	26.77	55.55	57.02	0.83

Table 6. The results for generalized zero-shot learning with alternate graph neural networks as class encoders.

Finally, to better understand the differences between GAT and TrGCN, we perform an ablation on GAT with more layers to increase the expressivity in the ZSL-KG framework. Table 7 shows that adding more layers to ZSL-KG-GAT hurts performance, while ZSL-KG with TrGCN achieves the highest performance. This suggests that the non-linear aggregator in TrGCN contributes to the difference in performance.

	AWA2	aPY
	H	H
ZSL-KG-GAT	73.35	60.91
ZSL-KG-GAT (2-layers)	72.68	60.72
ZSL-KG-GAT (3-layers)	71.71	60.65
ZSL-KG	74.58	61.57

Table 7. The results for generalized zero-shot learning on AWA2 and aPY datasets with graph attention networks.

5. Related Work

We broadly describe related works on zero-shot learning and graph neural networks.

Zero-Shot Learning. Zero-shot learning has been thoroughly researched in the computer vision community for object classification (Akata et al., 2015; Farhadi et al., 2009; Frome et al., 2013; Lampert et al., 2014; Wang et al., 2019; Xian et al., 2018; Min et al., 2020; Liu et al., 2021; Chou et al., 2021). Recent works in zero-shot learning have used graph neural networks for object classification (Kampffmeyer et al., 2019; Wang et al., 2018). In our work, we extend their approach to common sense knowledge graphs to generate class representations with a novel transformer graph convolutional network. HVE (Liu et al., 2020b) learns similarity between the image representation and the class representations in the hyperbolic space. However, the class representations are not learned with the task instead they are pretrained hyperbolic embeddings for GloVe and WordNet whereas in our work, we focus on methods that learn class representations explicitly from the knowledge graphs in the task. In another line of work, zero-shot object classification have used attention over image regions to achieve strong results on the task (Zhu et al., 2019; Liu et al., 2019b; Xie et al., 2019; Liu et al., 2020a). Our work focuses on the class encoder (TrGCN) learn attention over the graph rather the image region and could potentially complement methods that focus on image encoders. Finally, zero-shot fine-grained entity typing has been previously studied with a variety of class representations. ZOE (Zhou et al., 2018) is a specialized method for zero-shot fine-grained entity typing and shows accuracy competitive with supervised methods. It uses hand-crafted type definitions for each dataset and tuned thresholds, developed with knowledge of the unseen classes, which makes them a transductive zero-shot method. Our work focuses on graph-based methods in generalized zero-shot learning where unseen types are not revealed during training or tuning. Other notable works in zero-shot learning include text classification (Chang et al., 2008; Yin et al., 2019), video action recognition (Gan et al., 2015), machine translation (Johnson et al., 2017), and more (Wang et al., 2019).

Graph Neural Networks. Recent work on graph neural networks has demonstrated significant improvements for several downstream tasks such as node classification and graph classification (Hamilton et al., 2017a;b; Kipf & Welling, 2017; Veličković et al., 2018; Wu et al., 2019). Extensions of graph neural networks to relational graphs have produced significant results in several graph-related tasks (Marcheggiani & Titov, 2017; Schlichtkrull et al., 2018; Shang et al., 2019; Vashishth et al., 2020). Previous work has used transformers with graph neural networks as a method to generate meta-paths in the graph rather than as a neighbourhood aggregation technique (Yun et al., 2019). Finally, several diverse applications using graph neural networks have been explored: fine-grained entity typing (Xiong et al., 2019), text classification (Yao et al., 2019), reinforcement learning (Adhikari et al., 2020) and neural machine translation (Bastings et al., 2017). For a more in-depth review, we point readers to Wu et al. (2020).

Common Sense Knowledge Graphs. Common sense knowledge graphs have been applied to a range of tasks (Lin et al., 2019; Zhang et al., 2019b; Bhagavatula et al., 2019; Bosselut et al., 2019; Shwartz et al., 2020). A related work TGG (Zhang et al., 2019a) uses common sense knowledge graph and graph neural networks for zero-shot object classification. TGG learns to model seen-unseen relation with a graph neural network. Their framework is transductive as they require the knowledge of unseen classes during training and uses hand-crafted attributes. In contrast, ZSL-KG is an inductive framework which does not require explicit knowledge of the unseen classes during training and learn class representations from the common sense knowledge graph. Finally, ConceptNet has been used for transductive zero-shot text classification as shallow features for class representation (Zhang et al., 2019b) along with other knowledge sources such as pretrained embeddings and textual description, which differs from our work as we generate dense vector representation from ConceptNet with TrGCN.

6. Conclusion

ZSL-KG is a flexible framework for zero-shot learning with common sense knowledge graphs and can be adapted to a wide variety of tasks without requiring additional human effort. Our framework introduces a novel transformer graph convolutional network to learn rich representation from common sense knowledge graphs. Our work demonstrates that common sense knowledge graphs are a powerful source of high-level knowledge and can benefit a range of tasks.

Acknowledgements

We thank Yang Zhang for help preparing the Ontonotes dataset. We thank Roma Patel, Elaheh Raisi, and Charles Lovering for providing helpful feedback on our work. This material is based on research sponsored by Defense Advanced Research Projects Agency (DARPA) and Air Force Research Laboratory (AFRL) under agreement number FA8750-19-2-1006. The U.S. Government is authorized to reproduce and distribute reprints for Governmental purposes notwithstanding any copyright notation thereon. The views and conclusions contained herein are those of the authors and should not be interpreted as necessarily representing the official policies or endorsements, either expressed or implied, of Defense Advanced Research Projects Agency (DARPA) and Air Force Research Laboratory (AFRL) or the U.S. Government. We gratefully acknowledge support from Google. Disclosure: Stephen Bach is an advisor to Snorkel AI, a company that provides software and services for weakly supervised machine learning.

References

- Adhikari, A., Yuan, X., Côté, M.-A., Zelinka, M., Rondeau, M.-A., Laroche, R., Poupart, P., Tang, J., Trischler, A., and Hamilton, W. L. Learning dynamic knowledge graphs to generalize on text-based games. *arXiv preprint arXiv:2002.09127*, 2020.
- Akata, Z., Perronnin, F., Harchaoui, Z., and Schmid, C. Label-embedding for image classification. *IEEE Transactions on Pattern Analysis and Machine Intelligence (PAMI)*, 2015.
- Annadani, Y. and Biswas, S. Preserving semantic relations for zero-shot learning. *2018 IEEE/CVF Conference on Computer Vision and Pattern Recognition*, pp. 7603–7612, 2018.
- Ba, J. L., Kiros, J. R., and Hinton, G. E. Layer normalization. *arXiv preprint arXiv:1607.06450*, 2016.
- Bastings, J., Titov, I., Aziz, W., Marcheggiani, D., and Sima'an, K. Graph convolutional encoders for syntax-aware neural machine translation. *Proceedings of the 2017 Conference on Empirical Methods in Natural Language Processing (EMNLP)*, 2017.
- Bhagavatula, C., Le Bras, R., Malaviya, C., Sakaguchi, K., Holtzman, A., Rashkin, H., Downey, D., Yih, W.-t., and Choi, Y. Abductive commonsense reasoning. In *International Conference on Learning Representations*, 2019.
- Bosselut, A., Rashkin, H., Sap, M., Malaviya, C., Celikyilmaz, A., and Choi, Y. Comet: Commonsense transformers for automatic knowledge graph construction. *arXiv preprint arXiv:1906.05317*, 2019.
- Chang, M.-W., Ratnoff, L.-A., Roth, D., and Srikumar, V. Importance of semantic representation: Dataless classification. In *Aaai*, volume 2, pp. 830–835, 2008.
- Chao, W.-L., Changpinyo, S., Gong, B., and Sha, F. An empirical study and analysis of generalized zero-shot learning for object recognition in the wild. In *European conference on computer vision*, pp. 52–68. Springer, 2016.
- Chen, J., Ma, T., and Xiao, C. Fastgcn: fast learning with graph convolutional networks via importance sampling. *International Conference on Learning Representations (ICLR)*, 2018a.
- Chen, L., Zhang, H., Xiao, J., Liu, W., and Chang, S.-F. Zero-shot visual recognition using semantics-preserving adversarial embedding networks. In *CVPR*, 2018b.
- Chou, Y.-Y., Lin, H.-T., and Liu, T.-L. Adaptive and generative zero-shot learning. In *International Conference on Learning Representations*, 2021. URL <https://openreview.net/forum?id=ahAUv8TI2Mz>.
- Coucke, A., Saade, A., Ball, A., Bluche, T., Caulier, A., Leroy, D., Doumouro, C., Gisselbrecht, T., Caltagirone, F., Lavril, T., et al. Snips voice platform: an embedded spoken language understanding system for private-by-design voice interfaces. *ICML workshop on Privacy in Machine Learning and Artificial Intelligence*, 2018.
- Deng, J., Dong, W., Socher, R., Li, L.-J., Li, K., and Fei-Fei, L. Imagenet: A large-scale hierarchical image database. In *2009 IEEE conference on computer vision and pattern recognition*, pp. 248–255. Ieee, 2009.
- Durrett, G. and Klein, D. A joint model for entity analysis: Coreference, typing, and linking. *Transactions of the association for computational linguistics (TACL)*, 2014.
- Farhadi, A., Endres, I., Hoiem, D., and Forsyth, D. A. Describing objects by their attributes. *Proceedings of the IEEE Conference on Computer Vision and Pattern Recognition (CVPR)*, 2009.
- Frome, A., Corrado, G. S., Shlens, J., Bengio, S., Dean, J., Ranzato, M., and Mikolov, T. Devise: A deep visual-semantic embedding model. In *Advances in Neural Information Processing Systems (NeurIPS)*, 2013.
- Gan, C., Lin, M., Yang, Y., Zhuang, Y., and Hauptmann, A. G. Exploring semantic inter-class relationships (sir) for zero-shot action recognition. In *Proceedings of the AAAI Conference on Artificial Intelligence*, volume 29, 2015.

- Gardner, M., Grus, J., Neumann, M., Tafjord, O., Dasigi, P., Liu, N. F., Peters, M., Schmitz, M., and Zettlemoyer, L. S. Allennlp: A deep semantic natural language processing platform. 2017.
- Gillick, D., Lazic, N., Ganchev, K., Kirchner, J., and Huynh, D. Context-dependent fine-grained entity type tagging. *arXiv preprint arXiv:1412.1820*, 2014.
- Gupta, N., Lin, K., Roth, D., Singh, S., and Gardner, M. Neural module networks for reasoning over text. In *International Conference on Learning Representations (ICLR)*, 2020.
- Hamilton, W., Ying, Z., and Leskovec, J. Inductive representation learning on large graphs. In *Advances in Neural Information Processing Systems (NeurIPS)*, 2017a.
- Hamilton, W. L., Ying, R., and Leskovec, J. Representation learning on graphs: Methods and applications. *IEEE Data Engineering Bulletin*, 2017b.
- He, K., Zhang, X., Ren, S., and Sun, J. Deep residual learning for image recognition. In *Proceedings of the IEEE Conference on Computer Vision and Pattern Recognition (CVPR)*, 2016.
- Johnson, M., Schuster, M., Le, Q. V., Krikun, M., Wu, Y., Chen, Z., Thorat, N., Viégas, F., Wattenberg, M., Corrado, G., Hughes, M., and Dean, J. Google’s multilingual neural machine translation system: Enabling zero-shot translation. *Transactions of the Association for Computational Linguistics*, 5:339–351, 2017. doi: 10.1162/tacl.a.00065. URL <https://www.aclweb.org/anthology/Q17-1024>.
- Joshi, C. Transformers are graph neural networks. *The Gradient*, 2020.
- Kampffmeyer, M., Chen, Y., Liang, X., Wang, H., Zhang, Y., and Xing, E. P. Rethinking knowledge graph propagation for zero-shot learning. In *Proceedings of the IEEE Conference on Computer Vision and Pattern Recognition (CVPR)*, 2019.
- Keshari, R., Singh, R., and Vatsa, M. Generalized zero-shot learning via over-complete distribution. *2020 IEEE/CVF Conference on Computer Vision and Pattern Recognition (CVPR)*, pp. 13297–13305, 2020.
- Kingma, D. P. and Ba, J. Adam: A method for stochastic optimization. *International Conference on Learning Representations (ICLR)*, 2015.
- Kipf, T. N. and Welling, M. Semi-supervised classification with graph convolutional networks. In *International Conference on Learning Representations (ICLR)*, 2017.
- Kumar, A., Muddireddy, P. R., Dreyer, M., and Hoffmeister, B. Zero-shot learning across heterogeneous overlapping domains. *Proc. Interspeech 2017*, pp. 2914–2918, 2017.
- Lampert, C. H., Nickisch, H., and Harmeling, S. Attribute-based classification for zero-shot visual object categorization. *IEEE Transactions on Pattern Analysis and Machine Intelligence (PAMI)*, 2014.
- Li, K., Min, M. R., and Fu, Y. Rethinking zero-shot learning: A conditional visual classification perspective. *2019 IEEE/CVF International Conference on Computer Vision (ICCV)*, pp. 3582–3591, 2019.
- Lin, B. Y., Chen, X., Chen, J., and Ren, X. Kagnet: Knowledge-aware graph networks for commonsense reasoning. *Proceedings of the 2019 Conference on Empirical Methods in Natural Language Processing and the 9th International Joint Conference on Natural Language Processing (EMNLP-IJCNLP)*, 2019.
- Ling, X. and Weld, D. S. Fine-grained entity recognition. In *AAAI Conference on Artificial Intelligence (AAAI)*, 2012.
- Liu, H. and Singh, P. Conceptnet—a practical commonsense reasoning tool-kit. *BT technology journal*, 2004.
- Liu, H., Zhang, X., Fan, L., Fu, X., Li, Q., Wu, X.-M., and Lam, A. Y. Reconstructing capsule networks for zero-shot intent classification. In *Proceedings of the 2019 Conference on Empirical Methods in Natural Language Processing and the 9th International Joint Conference on Natural Language Processing (EMNLP-IJCNLP)*, 2019a.
- Liu, L., Zhou, T., Long, G., Jiang, J., and Zhang, C. Attribute propagation network for graph zero-shot learning. *Proceedings of the AAAI Conference on Artificial Intelligence*, 34:4868–4875, Apr. 2020a. doi: 10.1609/aaai.v34i04.5923. URL <https://ojs.aaai.org/index.php/AAAI/article/view/5923>.
- Liu, L., Zhou, T., Long, G., Jiang, J., Dong, X., and Zhang, C. Isometric propagation network for generalized zero-shot learning. In *International Conference on Learning Representations*, 2021. URL <https://openreview.net/forum?id=-mWcQVLPSPy>.
- Liu, S., Chen, J., Pan, L., Ngo, C.-W., Chua, T.-S., and Jiang, Y.-G. Hyperbolic visual embedding learning for zero-shot recognition. In *Proceedings of The Conference on Computer Vision and Pattern Recognition (CVPR)*, June 2020b.
- Liu, Y., Guo, J., Cai, D., and He, X. Attribute attention for semantic disambiguation in zero-shot learning. In *Proceedings of the IEEE International Conference on Computer Vision*, pp. 6698–6707, 2019b.

- Marcel, S. and Rodriguez, Y. Torchvision: The machine-vision package of torch. In *International Conference on Multimedia*, 2010.
- Marcheggiani, D. and Titov, I. Encoding sentences with graph convolutional networks for semantic role labeling. In *Proceedings of the 2017 Conference on Empirical Methods in Natural Language Processing (EMNLP)*, 2017.
- Mikolov, T., Sutskever, I., Chen, K., Corrado, G. S., and Dean, J. Distributed representations of words and phrases and their compositionality. In *Advances in Neural Information Processing Systems (NeurIPS)*, 2013.
- Min, S., Yao, H., Xie, H., Wang, C., Zha, Z.-J., and Zhang, Y. Domain-aware visual bias eliminating for generalized zero-shot learning. In *Proceedings of the IEEE/CVF Conference on Computer Vision and Pattern Recognition (CVPR)*, June 2020.
- Murphy, R. L., Srinivasan, B., Rao, V., and Ribeiro, B. Janossy pooling: Learning deep permutation-invariant functions for variable-size inputs. *International Conference on Learning Representations (ICLR)*, 2019.
- Narayan, S., Gupta, A., Khan, F., Snoek, C. G. M., and Shao, L. Latent embedding feedback and discriminative features for zero-shot classification. In *ECCV*, 2020.
- Obeidat, R., Fern, X., Shahbazi, H., and Tadepalli, P. Description-based zero-shot fine-grained entity typing. In *Proceedings of the 2019 Conference of the North American Chapter of the Association for Computational Linguistics: Human Language Technologies*, 2019.
- Pennington, J., Socher, R., and Manning, C. D. Glove: Global vectors for word representation. In *Proceedings of the 2014 conference on empirical methods in natural language processing (EMNLP)*, 2014.
- Reed, S., Akata, Z., Lee, H., and Schiele, B. Learning deep representations of fine-grained visual descriptions. In *Proceedings of the IEEE Conference on Computer Vision and Pattern Recognition (CVPR)*, June 2016.
- Ren, X., He, W., Qu, M., Huang, L., Ji, H., and Han, J. Afet: Automatic fine-grained entity typing by hierarchical partial-label embedding. In *Proceedings of the 2016 Conference on Empirical Methods in Natural Language Processing*, pp. 1369–1378, 2016.
- Romera-Paredes, B. and Torr, P. An embarrassingly simple approach to zero-shot learning. In *International Conference on Machine Learning (ICML)*, 2015.
- Russakovsky, O., Deng, J., Su, H., Krause, J., Satheesh, S., Ma, S., Huang, Z., Karpathy, A., Khosla, A., Bernstein, M., Berg, A. C., and Fei-Fei, L. ImageNet Large Scale Visual Recognition Challenge. *International Journal of Computer Vision (IJCV)*, 2015.
- Sabour, S., Frosst, N., and Hinton, G. E. Dynamic routing between capsules. In *Advances in Neural Information Processing Systems (NeurIPS)*, 2017.
- Schlichtkrull, M., Kipf, T. N., Bloem, P., Van Den Berg, R., Titov, I., and Welling, M. Modeling relational data with graph convolutional networks. In *European Semantic Web Conference*, 2018.
- Shang, C., Tang, Y., Huang, J., Bi, J., He, X., and Zhou, B. End-to-end structure-aware convolutional networks for knowledge base completion. In *AAAI Conference on Artificial Intelligence (AAAI)*, 2019.
- Shimaoka, S., Stenetorp, P., Inui, K., and Riedel, S. Neural architectures for fine-grained entity type classification. *Proceedings of the 15th Conference of the European Chapter of the Association for Computational Linguistics: Volume 1, Long Papers (EACL)*, 2017.
- Shwartz, V., West, P., Le Bras, R., Bhagavatula, C., and Choi, Y. Unsupervised commonsense question answering with self-talk. In *Proceedings of the 2020 Conference on Empirical Methods in Natural Language Processing (EMNLP)*, pp. 4615–4629, 2020.
- Skorokhodov, I. and Elhoseiny, M. Class normalization for zero-shot learning. In *International Conference on Learning Representations*, 2021. URL <https://openreview.net/forum?id=7pgFL2Dkyyy>.
- Socher, R., Ganjoo, M., Manning, C. D., and Ng, A. Zero-shot learning through cross-modal transfer. In *Advances in Neural Information Processing Systems (NeurIPS)*, 2013.
- Speer, R., Chin, J., and Havasi, C. Conceptnet 5.5: An open multilingual graph of general knowledge. In *AAAI Conference on Artificial Intelligence (AAAI)*, 2017.
- Sung, F., Yang, Y., Zhang, L., Xiang, T., Torr, P., and Hospedales, T. M. Learning to compare: Relation network for few-shot learning. *2018 IEEE/CVF Conference on Computer Vision and Pattern Recognition*, pp. 1199–1208, 2018.
- Tandon, N., De Melo, G., and Weikum, G. Webchild 2.0: Fine-grained commonsense knowledge distillation. In *Proceedings of ACL 2017, System Demonstrations*, 2017.
- Vashishth, S., Sanyal, S., Nitin, V., and Talukdar, P. Composition-based multi-relational graph convolutional networks. In *International Conference on Learning Representations (ICLR)*, 2020.

- Vaswani, A., Shazeer, N., Parmar, N., Uszkoreit, J., Jones, L., Gomez, A. N., Kaiser, Ł., and Polosukhin, I. Attention is all you need. In *Advances in Neural Information Processing Systems (NeurIPS)*, 2017.
- Veličković, P., Cucurull, G., Casanova, A., Romero, A., Lio, P., and Bengio, Y. Graph attention networks. *International Conference on Learning Representations (ICLR)*, 2018.
- Verma, V. K., Brahma, D., and Rai, P. A meta-learning framework for generalized zero-shot learning. *AAAI Conference on Artificial Intelligence (AAAI)*, 2020.
- Vyas, M. R., Venkateswara, H., and Panchanathan, S. Leveraging seen and unseen semantic relationships for generative zero-shot learning. In *ECCV*, 2020.
- Wang, W., Zheng, V. W., Yu, H., and Miao, C. A survey of zero-shot learning: Settings, methods, and applications. *ACM Transactions on Intelligent Systems and Technology (TIST)*, 2019.
- Wang, X., Ye, Y., and Gupta, A. Zero-shot recognition via semantic embeddings and knowledge graphs. *Proceedings of the IEEE Conference on Computer Vision and Pattern Recognition (CVPR)*, 2018.
- Weischedel, R. and Brunstein, A. Bbn pronoun coreference and entity type corpus. *Linguistic Data Consortium, Philadelphia*, 112, 2005.
- Wu, F., Zhang, T., Souza Jr, A. H. d., Fifty, C., Yu, T., and Weinberger, K. Q. Simplifying graph convolutional networks. *International Conference on Machine Learning (ICML)*, 2019.
- Wu, Z., Pan, S., Chen, F., Long, G., Zhang, C., and Philip, S. Y. A comprehensive survey on graph neural networks. *IEEE Transactions on Neural Networks and Learning Systems*, 2020.
- Xia, C., Zhang, C., Yan, X., Chang, Y., and Yu, P. S. Zero-shot user intent detection via capsule neural networks. *Proceedings of the 2018 Conference on Empirical Methods in Natural Language Processing*, 2018.
- Xian, Y., Akata, Z., Sharma, G., Nguyen, Q., Hein, M., and Schiele, B. Latent embeddings for zero-shot classification. In *Proceedings of the IEEE Conference on Computer Vision and Pattern Recognition*, 2016.
- Xian, Y., Lampert, C. H., Schiele, B., and Akata, Z. Zero-shot learning—a comprehensive evaluation of the good, the bad and the ugly. *IEEE Transactions on Pattern Analysis and Machine Intelligence (PAMI)*, 2018.
- Xie, G.-S., Liu, L., Jin, X., Zhu, F., Zhang, Z., Qin, J., Yao, Y., and Shao, L. Attentive region embedding network for zero-shot learning. In *Proceedings of the IEEE Conference on Computer Vision and Pattern Recognition*, pp. 9384–9393, 2019.
- Xiong, W., Wu, J., Lei, D., Yu, M., Chang, S., Guo, X., and Wang, W. Y. Imposing label-relational inductive bias for extremely fine-grained entity typing. *Proceedings of the 2019 Conference of the North American Chapter of the Association for Computational Linguistics: Human Language Technologies, Volume 1 (Long and Short Papers) (NAACL)*, 2019.
- Xu, K., Hu, W., Leskovec, J., and Jegelka, S. How powerful are graph neural networks? In *International Conference on Learning Representations (ICLR)*, 2019.
- Xu, W., Xian, Y., Wang, J., Schiele, B., and Akata, Z. Attribute prototype network for zero-shot learning. *ArXiv*, abs/2008.08290, 2020.
- Yaghoobzadeh, Y. and Schütze, H. Corpus-level fine-grained entity typing using contextual information. *Proceedings of the 2015 Conference on Empirical Methods in Natural Language Processing (EMNLP)*, 2015.
- Yao, L., Mao, C., and Luo, Y. Graph convolutional networks for text classification. In *AAAI Conference on Artificial Intelligence (AAAI)*, 2019.
- Yavuz, S., Gur, I., Su, Y., Srivatsa, M., and Yan, X. Improving semantic parsing via answer type inference. In *Proceedings of the 2016 Conference on Empirical Methods in Natural Language Processing (EMNLP)*, 2016.
- Yin, W., Hay, J., and Roth, D. Benchmarking zero-shot text classification: Datasets, evaluation and entailment approach. In *Proceedings of the 2019 Conference on Empirical Methods in Natural Language Processing and the 9th International Joint Conference on Natural Language Processing (EMNLP-IJCNLP)*, 2019.
- Ying, R., He, R., Chen, K., Eksombatchai, P., Hamilton, W. L., and Leskovec, J. Graph convolutional neural networks for web-scale recommender systems. In *Proceedings of the 24th ACM SIGKDD International Conference on Knowledge Discovery & Data Mining*, 2018.
- Yogatama, D., Gillick, D., and Lazic, N. Embedding methods for fine grained entity type classification. In *Proceedings of the 53rd Annual Meeting of the Association for Computational Linguistics and the 7th International Joint Conference on Natural Language Processing (Volume 2: Short Papers)*, 2015.

- Yu, Y., Ji, Z., Han, J., and Zhang, Z. Episode-based prototype generating network for zero-shot learning. In *2020 IEEE/CVF Conference on Computer Vision and Pattern Recognition (CVPR)*, pp. 14032–14041, 2020. doi: 10.1109/CVPR42600.2020.01405.
- Yuan, Z. and Downey, D. Otyper: A neural architecture for open named entity typing. In *AAAI Conference on Artificial Intelligence (AAAI)*, 2018.
- Yun, S., Jeong, M., Kim, R., Kang, J., and Kim, H. J. Graph transformer networks. In *Advances in Neural Information Processing Systems*, pp. 11960–11970, 2019.
- Zhang, C., Lyu, X., and Tang, Z. Tgg: Transferable graph generation for zero-shot and few-shot learning. In *Proceedings of the 27th ACM International Conference on Multimedia*, pp. 1641–1649, 2019a.
- Zhang, H., Khashabi, D., Song, Y., and Roth, D. Transoms: From linguistic graphs to commonsense knowledge. *Proceedings of International Joint Conference on Artificial Intelligence (IJCAI)*, 2020.
- Zhang, J., Lertvittayakumjorn, P., and Guo, Y. Integrating semantic knowledge to tackle zero-shot text classification. In *Proceedings of the 2019 Conference of the North American Chapter of the Association for Computational Linguistics: Human Language Technologies, Volume 1 (Long and Short Papers)*, 2019b.
- Zhao, B., Fu, Y., Liang, R., Wu, J., Wang, Y., and Wang, Y. A large-scale attribute dataset for zero-shot learning. In *Proceedings of the IEEE Conference on Computer Vision and Pattern Recognition Workshops*, 2019.
- Zhou, B., Khashabi, D., Tsai, C.-T., and Roth, D. Zero-shot open entity typing as type-compatible grounding. In *EMNLP*, 2018.
- Zhu, Y., Xie, J., Tang, Z., Peng, X., and Elgammal, A. Semantic-guided multi-attention localization for zero-shot learning. In *Advances in Neural Information Processing Systems*, pp. 14943–14953, 2019.

A. LSTM Predictions

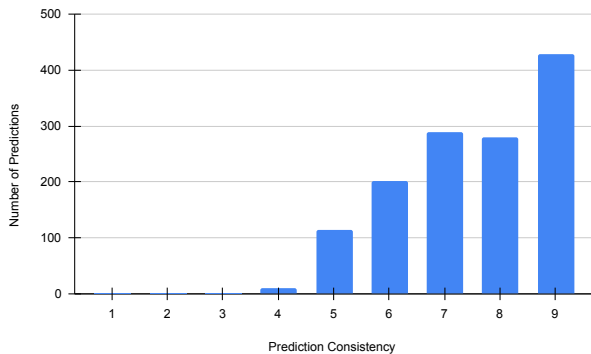


Figure 2. Graph showing distribution of inconsistencies in the LSTM-based aggregator predictions.

LSTMs have been used in graph neural networks as aggregators to generate more expressive node embeddings. However, LSTMs assume an ordering of the inputs which is not present in a graph neighbourhood. To apply LSTMs to an unordered set of nodes, (Hamilton et al., 2017a) randomly permute the nodes in the neighbourhood.

We test whether randomly permuting the node neighbours makes LSTM-based aggregator permutation invariant. We replicate the LSTM-based aggregator to work with the ZSL-KG framework. The model is trained with the setup described in Section 4.2. We run the prediction on the Animals with Attributes 2 dataset by computing 10 class representation for each of the classes using the trained LSTM-based aggregator model.

The experiments reveal that 1325 out of 7913 (16.78%) have multiple predictions for the same image in the unseen classes. For images that have multiple predictions, we take the count of the mode prediction and plot the histogram. Figure 2 shows inconsistency in predictions. The graph for a given value p on the x-axis is read as for every 10 prediction, p times the same output is predicted.

B. ConceptNet Setup

In all our experiments with ZSL-KG, we map each class to a node in ConceptNet 5.7 (Speer et al., 2017) and query its 2-hop neighbourhood. Next, we post-process all We remove all the non-English concepts and their edges from the graph and make all the edges bidirectional. Then, we take the union of the concepts’ neighbourhood that share the same prefix. For example, we take the union of the /c/en/elephant and /c/en/elephant/n. Then, we compute the embeddings for the concept using the pre-trained 300 dimensional GloVe 840B (Pennington et al., 2014). We average the individual word in the concept to

get the embedding. These embeddings serve as initial features for the graph neural network. For the random walk, the number of steps is 20, and the number of restarts is 10. We add one smoothing to the visit counts and normalize the counts for the neighboring nodes. During training, we sample K neighbours with the highest hitting probabilities at each hop. For OntoNotes, BBN, AWA2, and aPY we sample 50 neighbours in the first hop and 100 neighbours in the second hop. For ImageNet we sample 100 and 200 neighbours in the first and second hop.

C. Pseudocode

Algorithm 1 Forward pass with the ZSL-KG framework

input example x , example encoder $\theta(x)$, linear layer \mathbf{W} , class encoder $\phi(y)$, graph $\mathcal{G}(V, E, R)$, class nodes $\{v_y^1, v_y^2, \dots, v_y^n\}$, node initialization $\mathbf{H} = [h^0, \dots, h^v]$, depth L , graph neural network weights $\{\mathbf{W}^1, \dots, \mathbf{W}^L\}$, transformers $\{T^1, \dots, T^L\}$, neighbourhood sample sizes $\{s^1, \dots, s^L\}$

output logits for classes $y = \{y_1, y_2, \dots, y_n\}$

function TrGCN $\{V, l = 0\}$

if $l = L$ **then**

return $\mathbf{H}_V \leftarrow \mathbf{H}(V)$

else

$i \leftarrow 0$

for $v \in V$ **do**

$N \leftarrow \mathcal{N}(v, s^{l+1})$

$\mathbf{H}_N \leftarrow \text{TrGCN}\{N, l + 1\}$

$\mathbf{Z}_N \leftarrow T^{(l+1)}(\mathbf{H}_N)$

$\mathbf{a}_v^{(l+1)} \leftarrow \text{mean}(\mathbf{Z}_N)$

$\mathbf{h}_v^{(l+1)} \leftarrow \sigma(\mathbf{W}^{(l+1)} \cdot \mathbf{a}_v)$

$\mathbf{H}_i^{(l+1)} = \mathbf{h}_v^{(l+1)} / \|\mathbf{h}_v^{(l+1)}\|_2$

$i \leftarrow i + 1$

end for

return $\mathbf{H}^{(l+1)}$

end if

end function

$\phi(y) \leftarrow \text{TrGCN}\{\{v_y^1, v_y^2, \dots, v_y^n\}, L\}$

return $\theta(x)^T \mathbf{W} \phi(y)$

In Algorithm 1, we describe the forward pass with the ZSL-KG framework. TrGCN computes the class representations for the nodes in the graph. The class representations are used in the bilinear similarity function to compute the compatibility scores for the classes.

D. Dataset Details

Here, we provide details about the datasets used in our experiments.

Table 8 shows the statistics for fine-grained entity typing

Dataset	Seen classes	Unseen classes	Train examples	Test examples
OntoNotes	40	32	220398	9604
BBN	15	24	85545	12349

Table 8. Zero-shot fine-grained entity typing datasets used in our experiments.

Dataset	Seen classes	Unseen classes	Seen examples	Seen test examples	Unseen test examples
AWA2	40	10	23527	5882	7913
aPY	20	12	5932	1483	7924

Table 9. Zero-shot object classification datasets used in our experiments.

datasets. We obtain the OntoNotes and BBN dataset from Ren et al. (2016). OntoNotes has three levels of types such as `/location`, `/location/structure`, `/location/structure/government` where `/location` and `/location/structure` are treated as coarse-grained entity types and `/location/structure/government` is treated as fine-grained entity type. Similarly, BBN has two levels of types and we consider the level two types as fine-grained types. Furthermore, we process the datasets by removing all the fine-grained entity types from the train set. We also remove all the examples from the train set where coarse-grained entity types are not present in the test set. We note that the OntoNotes dataset has `/other` type which cannot be mapped to a meaningful concept or a wikipedia article. Since `/other` is a coarse-grained entity type, we train a weight vector for the type and treat as class representation.

Table 9 shows statistics for object classification datasets. Our work follows the proposed splits suggested in Xian et al. (2018). Since aPY has multiple objects in an image, we crop objects with the bounding box information provided and use the cropped images for training and testing. Apart from AWA2 and aPY, we evaluate ZSL-KG on the ImageNet dataset. ImageNet dataset has a total of 1000 seen classes and 20842 unseen classes.

E. Experiment Details

E.1. Fine-grained Entity Typing

We reconstruct OType (Yuan & Downey, 2018) and DZET (Obeidat et al., 2019) for fine-grained entity typing. OType averages the 300 dimensional GloVe 840B embeddings for the tokens in the entity type or the class. For DZET, we manually mapped the classes to Wikipedia articles. We pass each article’s first paragraph through a learnable biLSTM with attention to learn the class representations (Appendix F).

For both OntoNotes and BBN, the methods are trained for 5 epochs by minimizing the cross-entropy loss using Adam with a learning rate 0.001. During inference, we pass the scores from the bilinear similarity model through a sigmoid and pick the labels that have probability of 0.5 or greater as our prediction. Since we have coarse-grained types along with fine grained types, we set calibration coefficient γ to 0.

E.2. Object Classification

For the ImageNet experiment, we train ZSL-KG by minimizing the L2 distance between the learned class representations and the weights fully connected layer of a ResNet50 classifier for 3000 epochs on 1000 classes from the ILSVRC 2012. Similar to DGP and SGCN, we freeze the class representations for the class representations and fine-tune the ResNet-backbone on the ILSVRC 2012 dataset for 20 epochs using SGD with a learning rate 0.0001 and momentum of 0.9. During inference, we switch the knowledge graph to the ImageNet graph and generate class representations from them. For fair comparison with other graph-based methods on ImageNet, we use ResNet50 model (He et al., 2016) in Torchvision (Marcel & Rodriguez, 2010) pretrained on ILSVRC 2012 (Russakovsky et al., 2015) and do not calibrate the outputs from ZSL-KG.

For AWA2 and aPY, we follow the same L2 training scheme and train for 1000 epochs on 950 random classes from 1000 ILSVRC 2012 classes, while the remaining 50 classes are used for validation. The model with the least loss on the validation classes is used to generate the seen and unseen class representations with the graph. Since only a subset of the seen classes for AWA2 (22 out of 40) and aPY (2 out of 20) are part of ILSVRC 2012 classes, we freeze the class representations for the seen classes and fine-tune a pretrained ResNet101-backbone on the individual datasets for 25 epochs using SGD with a learning rate 0.0001 and momentum of 0.9. We calibrate γ on the validation splits as suggested in Xian et al. (2018) and set $\gamma = 3.0$ for AWA2 and $\gamma = 2.0$ for aPY for all the methods.

	AWA2				aPY			
	T1	U	S	H	T1	U	S	H
SP-AEN (Chen et al., 2018b)	58.5	23.3	90.9	37.1	24.1	13.7	63.4	22.6
PSR (Annadani & Biswas, 2018)	63.8	20.7	73.8	32.3	38.4	13.5	51.4	21.4
LFGAA+Hibrid (Liu et al., 2019b)	68.1	27.0	93.4	41.9	-	-	-	-
Relation Net (Sung et al., 2018)	64.2	30.0	93.4	45.3	-	-	-	-
f-VAEGAN-D2 (Xie et al., 2019)	70.3	57.1	76.1	65.2	-	-	-	-
LsrGAN (Vyas et al., 2020)	-	54.6	74.6	63.0	-	-	-	-
TF-VAEGAN (Narayan et al., 2020)	73.4	55.5	83.6	66.7	-	-	-	-
OCD-CVAE (Keshari et al., 2020)	71.3	59.5	73.4	65.7	-	-	-	-
GXE (Li et al., 2019)	71.1	56.4	81.4	66.7	38.0	26.5	74.0	39.0
E-PGN (Yu et al., 2020)	73.4	52.6	83.5	64.6	-	-	-	-
AREN (Xie et al., 2019)	66.9	54.7	79.1	64.7	39.2	30.0	47.9	36.9
ZSML (Verma et al., 2020)	77.5	58.9	74.6	65.8	64.0	36.3	46.6	40.9
DBVE (Min et al., 2020)	-	62.7	77.5	69.4	-	37.9	55.9	45.2
APN (Xu et al., 2020)	71.7	62.2	69.5	65.6	-	-	-	-
IPN (Liu et al., 2021)	-	67.5	79.2	72.9	-	37.2	66	47.6
CN-ZSL (Skorokhodov & Elhoseiny, 2021)	-	60.2	77.1	67.6	-	-	-	-
AGZSL (Chou et al., 2021)	76.4	69.0	86.5	76.8	43.7	36.2	58.6	44.8
ZSL-KG (ours)	78.1	66.8	84.4	74.6	60.5	55.2	69.7	61.6

Table 10. ZSL-KG compared to attribute-based zero-shot learning methods.

F. BiLSTM with Attention

The biLSTM with attention is used to learn class representations in DZET (Obeidat et al., 2019). The input tokens $w = w_0, w_1, \dots, w_n$ represented by 300 dimension GloVe 840B embeddings are passed to the biLSTM to get the hidden states \overrightarrow{h} and \overleftarrow{h} . The hidden states are concatenated to get $h = h_0, h_1, \dots, h_n$. Next, they are passed to the attention module to get the scalar attention values:

$$\alpha_i = W_\alpha (\tanh(W_e \cdot h_i)) \quad (9)$$

The scalar attention values are then normalized to with a softmax layer:

$$a_i = \frac{\exp(\alpha_i)}{\sum_i \exp(\alpha_i)} \quad (10)$$

The normalized scalar attention values are multiplied with their respective hidden vectors to get the final representation t_w :

$$t_w = \sum_{i=0}^n a_i h_i \quad (11)$$

G. AttentiveNER

Here, we describe AttentiveNER (Shimaoka et al., 2017) used as the example encoder in the fine-grained entity typing task. Each mention m comprises of n tokens mapped to a pretrained word embedding from GloVe 840B. We average

the embeddings to obtain a single vector v_m :

$$v_m = \frac{1}{n} \sum_{j=1}^n m_j \quad (12)$$

where $m_j \in \mathbb{R}^d$ is the pretrained embedding.

We learn the context of the mention using two biLSTM with attention layers. The left context l is represented by $\{l_1, l_2, \dots, l_s\}$ and the right context r by $\{r_1, r_2, \dots, r_s\}$ where $l_i \in \mathbb{R}^d$ and $r_j \in \mathbb{R}^d$ are the pretrained word embeddings for the left and the right context. We consider a context window size of s . We pass l and r through their separate biLSTM layers to get the hidden states $\overleftarrow{h}_l, \overrightarrow{h}_l$ for the left context and $\overleftarrow{h}_r, \overrightarrow{h}_r$ for the right context. The hidden states are passed through the attention layer to compute the attention scores. The attention layer is a two-layer feedforward neural network and computes the normalized attention for each of the hidden states $v_c \in \mathbb{R}^h$:

$$\alpha_i^l = W_\alpha (\tanh(W_e \begin{bmatrix} \overleftarrow{h}_i^l \\ \overrightarrow{h}_i^l \end{bmatrix})) \quad (13)$$

$$a_i^l = \frac{\exp(\alpha_i^l)}{\sum_i \exp(\alpha_i^l) + \sum_j \exp(\alpha_j^r)} \quad (14)$$

The scalar values are multiplied with their respective hidden states to get the final context vector representation v_c :

$$v_c = \sum_{i=0}^s a_i^l h_i^l + \sum_{j=0}^s a_j^r h_j^r \quad (15)$$

Finally, we concatenate the context vector v_c and v_m to get the example representation x .

H. Fine-grained entity typing evaluation

We follow the standard evaluation metric introduced in (Ling & Weld, 2012): Strict Accuracy, Loose Micro F1 and Loose Macro F1.

We denote the set of ground truth types as T and the set of predicted types as P . We use the F1 computed from the precision p and recall r for the evaluation metrics mentioned below:

Strict Accuracy. The prediction is considered correct if and only if $t_e = \hat{t}_e$:

$$p = \frac{\sum_{e \in P \cap T} \mathbf{1}(t_e = \hat{t}_e)}{|P|} \quad (16)$$

$$r = \frac{\sum_{e \in P \cap T} \mathbf{1}(t_e = \hat{t}_e)}{|T|} \quad (17)$$

Loose Micro. The precision and recall scores are computed as:

$$p = \frac{\sum_{e \in P} |t_e \cap \hat{t}_e|}{\sum_{e \in P} |\hat{t}_e|} \quad (18)$$

$$r = \frac{\sum_{e \in T} |t_e \cap \hat{t}_e|}{\sum_{e \in T} |\hat{t}_e|} \quad (19)$$

Loose Macro. The precision and recall scores are computed as:

$$p = \frac{1}{|P|} \sum_{e \in P} \frac{|t_e \cap \hat{t}_e|}{|\hat{t}_e|} \quad (20)$$

$$r = \frac{1}{|T|} \sum_{e \in T} \frac{|t_e \cap \hat{t}_e|}{|\hat{t}_e|} \quad (21)$$

I. Results on AWA2 and aPY

Table 10 shows results comparing ZSL-KG with other related work from zero-shot object classification.

J. Intent Classification

To assess ZSL-KG’s versatility, we experiment on zero-shot intent classification. Intent classification is a text classification task of identifying users’ intent expressed in chatbots and personal voice assistants.

Finally, we concatenate the context vector v_c and v_m to get the example representation x .

Dataset. We evaluate on the main open-source benchmark for intent classification: SNIPS-NLU (Coucke et al., 2018).

	SNIPS-NLU
	Accuracy
Zero-shot DNN	71.16
IntentCapsNet	77.52
ReCapsNet-ZS	79.96
GCNZ	82.47 ± 03.09
SGCN	50.27 ± 14.13
DGP	64.41 ± 12.87
ZSL-KG	88.98 ± 01.22

Table 11. Results for intent classification on the SNIPS-NLU dataset. We report the average accuracy of the models on 5 random seeds and the standard error. The results for Zero-shot DNN, IntentCapsNet, and ReCapsNet-ZS are obtained from Liu et al. (2019a).

The dataset was collected using crowdsourcing to benchmark the performance of voice assistants. The training set has 5 seen classes which we split into 3 train classes and 2 development classes.

Experiment. Zero-shot intent classification is a multi-class classification task. The example encoder used in our experiments is a biLSTM with attention (Appendix F). We train the model for 10 epochs by minimizing the cross entropy loss and pick the model with the least loss on the development set. We measure accuracy on the test classes.

We compare ZSL-KG against existing specialized state-of-the-art methods in the literature for zero-shot intent classification: Zero-shot DNN (Kumar et al., 2017), IntentCapsNet (Xia et al., 2018), and ResCapsNet-ZS (Liu et al., 2019a). IntentCapsNet and ResCapsNet-ZS are CapsuleNet-based (Sabour et al., 2017) approaches and have reported the best performance on the task.

Results. Table 11 shows the results. ZSL-KG significantly outperforms the existing approaches and improves the state-of-the-art accuracy to 88.98%. The graph-based methods have mixed performance on intent classification and suggests ZSL-KG works well on a broader range of tasks.

K. Graph Neural Networks Architecture Details

Table 12 describes the aggregator and combine function for the ablation experiments. ZSL-KG-GCN uses a mean aggregator to learn the neighbourhood structure. ZSL-KG-GAT projects the neighbourhood nodes to a new features $h_u^{(l-1)} = W h_u^{(l-1)}$. The neighbourhood node features are concatenated with self feature and passed through a self-attention module for get the attention coefficients. The attention coefficients are multiplied with the neighbourhood

<i>Method</i>	<i>Aggregate</i>	<i>Combine</i>
ZSL-KG-GCN	$\mathbf{a}_v^{(l)} = \text{Mean} \left(\left\{ \mathbf{h}_u^{(l-1)}, u \in \mathcal{N}(v) \right\} \right)$	$\mathbf{h}_v^{(l)} = \sigma \left(\mathbf{W}^{(l)} \mathbf{a}_v^{(l)} \right)$
ZSL-KG-GAT	$\alpha_u^{(l)} = \text{Attn} \left(\left\{ \mathbf{h}_u^{(l-1)} \parallel \mathbf{h}^{(l-1)} \right\}_v, u \in \mathcal{N}(v) \right)$	$\mathbf{h}_v^{(l)} = \sigma \left(\sum_{u=1}^{\mathcal{N}(v)+1} \alpha_u^{(l)} \mathbf{h}_u^{(l-1)} \right)$
ZSL-KG-RGCN	$\mathbf{a}_v^{(l)} = \sum_{r \in R} \sum_{j \in \mathcal{N}(v)^r} \frac{1}{c_{i,r}} \sum_{b \in B} \alpha_{b,r}^{(l)} \mathbf{V}_b^{(l)} \mathbf{h}_j^{(l-1)}$	$\mathbf{h}_v = \sigma \left(\mathbf{a}_v + \mathbf{W}_s^{(l)} \mathbf{h}_v^{(l-1)} \right)$
ZSL-KG-LSTM	$\mathbf{a}_v^{(l)} = \text{LSTM}^{(l)} \left(\mathbf{h}_u^{(l-1)} \forall u \in \mathcal{N}(v) \right)$	$\mathbf{h}_v^{(l)} = \sigma \left(\mathbf{W} \cdot [\mathbf{h}_v^{(l-1)} \parallel \mathbf{a}_v^{(l)}] \right)$

Table 12. Graph Aggregators

	<i>AWA2</i>	<i>aPY</i>	<i>SNIPS-NLU</i>
	T1	T1	Accuracy
ZSL-KG	78.08 ± 0.84	64.36 ± 0.59	88.98 ± 1.22
-GCN	74.81 ± 0.93	61.63 ± 0.54	84.78 ± 0.77
-GAT	75.29 ± 0.64	62.87 ± 0.36	87.57 ± 1.59
-RGCN	66.27 ± 1.01	54.20 ± 0.63	87.47 ± 1.81
-LSTM	66.46 ± 1.19	54.89 ± 0.74	88.81 ± 1.17

Table 13. The results for zero-shot learning tasks with other graph neural networks. We report the average performance on 5 random seeds and the standard error.

features to the get the node embedding for the l -th layer in the combine function. ZSL-KG-RGCN uses a relational aggregator to learn the structure of the neighbourhood. To avoid overparameterization from the relational weights, we perform basis decomposition of the weight vector into B bases. We learn $|B|$ relational coefficients and $|B|$ weight vectors in the aggregate function and add with the self feature in combine function. ZSL-KG-LSTM uses LSTM as an aggregator to combine the neighbourhood features. The nodes in the graph are passed through an LSTM and the last hidden state is taken as the aggregated vector. The aggregated vector is concatenated with the node’s previous layer feature and passed to the combine function to get the node representation.

L. Comparison of Graph Aggregators on ZSL

Similar to Table 13 shows results for zero-shot learning, where only unseen classes are present during testing. Our results show that ZSL-KG significantly outperforms other graph neural networks on object classification and intent classification datasets.

M. Hyperparameters

In this section, we detail the hyperparameters used in our experiments.

M.1. Training Details

Our framework is built using PyTorch and AllenNLP (Gardner et al., 2017). In all our experiments, we use Adam (Kingma & Ba, 2015) to train our parameters with a learning rate of 0.001, unless provided in the experiments. During training, we set the weight decay to $5e - 04$ for OntoNotes, ImageNet, AWA2, and aPY and 0.0 for BBN. We set the weight decay to 0.0 when fine-tuning the ResNet backbone with SGD for ImageNet, AWA2, and aPY.

For fine-grained entity typing, we assume a low-rank for the compatibility matrix \mathbf{W} . The matrix $\mathbf{W} \in \mathbb{R}^{d_e \times d_c}$ is factorized into $\mathbf{A} \in \mathbb{R}^{h \times d_e}$ and $\mathbf{B} \in \mathbb{R}^{d_c \times h}$ where d_e is the size of example representation, d_c is the size of the the class representation, and h is the size of the joint semantic space. Following prior work (Obeidat et al., 2019), we set $h = 20$ as the size of the joint semantic space for all the experiments.

M.2. Graph Aggregator Summary

<i>Task</i>	<i>layer-1</i>	<i>layer-2</i>
Object classification	2048	2049
Fine-grained entity typing	128	128

Table 14. Output dimensions for the layers in the graph neural networks.

Table 14 details the output dimensions for the graph neural network layers. ZSL-KG-GCN, DGP, GCNZ, and SGN are linear aggregators and learn only one weight matrix in each of the layers. ZSL-KG-GAT learns a weight matrix for the attention where $\mathbf{W}_a \in \mathbb{R}^{2d_{(1)} \times 1}$ and uses LeakyReLU activation in the attention. LeakyReLU has a negative slope of 0.2. ZSL-KG-RGCN learns B bases weight vectors in the baseline. We found that $B = 1$ performs the best for fine-grained entity typing and object classification. In fine-grained entity typing, the activation function after the graph neural network layer is ReLU and following prior work in object classification, the activation function is LeakyReLU

with a negative slope of 0.2.

	<i>layer 1</i>		<i>layer 2</i>	
	$d_{(f)}$	$d_{(p)}$	$d_{(f)}$	$d_{(p)}$
OntoNotes	150	150	32	64
BBN	250	150	32	64
ImageNet	150	150	1024	1024
AWA2/aPY	100	150	1024	1024

Table 15. The hyperparameters used in our transformer graph convolutional network.

ZSL-KG with the transformer graph convolutional network is a complex architecture with numerous parameters. In our transformer module, there are five hyperparameters - input dimension $d_{(l-1)}$, output dimension $d_{(l-1)}$, feedforward layer hidden dimension $d_{(f)}$, and projection dimension $d_{(p)}$. The input dimension and output dimensions are the same in the aggregator. Table 15 details the hyperparameters used in our transformer graph convolutional networks. For fine-grained entity typing, we manually tuned the hyperparameters. We tuned the hyperparameters on the held-out validation classes for object classification.